Journal of Solid State Chemistry **153,** 140–144 (2000)
doi:10.1006/jssc.2000.8763, available online at http://www.idealibrary.com on IDEAL®

Charge Ordering and Magnetotransport Transitions in $Sm_{1/3}Sr_{2/3}FeO_{3-\delta}$

Y. M. Zhao, M. Hervieu,[1] N. Nguyen, and B. Raveau

Laboratoire CRISMAT, UMR 6508 associée au CNRS, ISMRA et Université de Caen, 6, Boulevard du Maréchal Juin, 14050 Caen Cedex, France

Received March 7, 2000; in revised form April 24, 2000; accepted May 5, 2000; published online July 7, 2000

Charge ordering (CO) between Fe^{3+} and Fe^{5+} species and magnetotransport transition have been shown for the first time in the perovskite $Sm_{1/3}Sr_{2/3}FeO_{3-\delta}$ by electron diffraction microscopy, by ^{57}Fe Mössbauer spectroscopy, and by measurements of transport and magnetic properties. This compound is charge ordered at $T_{CO} = 110$ K, which is significantly lower than the temperature $T_N = 150$ K of the magnetotransport transition. A charge disproportionation $2Fe^{4+} \leftrightarrow Fe^{3+} + Fe^{5+}$ is evidenced by Mössbauer spectroscopy. The electron diffraction study shows the coexistence of orthorhombic and rhombohedral-type domains. A comparison with the other lanthanides (La, Pr, Nd) is also made. This suggests that the size of the Ln^{3+} ion is not the only parameter which governs the charge ordering in these perovskites, but the oxygen stoichiometry, which influences the Fe^{5+} formation, may also play a role in the CO phenomenon. © 2000 Academic Press

Key Words: **samarium-based iron perovskite; charge ordering and magnetotransport transition; electron diffraction and ^{57}Fe Mössbauer studies; resistivity and magnetic measurements.**

INTRODUCTION

Transition metal oxides with the perovskite structure, which show strong electron correlations, have been subject of numerous investigations in recent years due to their extraordinary physical properties, such as high-T_C superconductivity in cuprates or colossal magnetoresistance in manganites (for a review see refs. 1 and 2). The metal–insulator transitions that appear in a number of these oxides are fascinating features where charge and orbital ordering or disordering have a role of prime importance.

In contrast to copper and manganese oxides, iron oxides with the perovskite structure have not been so extensively studied, perhaps because of their less spectacular properties. Nevertheless, the perovskite $La_{1-x}Sr_xFeO_3$, first studied by Waugh (3), is of the highest interest if one bears in mind the charge disproportionation of iron shown by Takano *et al.* (4) for the perovskite $La_{1/3}Sr_{2/3}FeO_3$. Using Mössbauer spectroscopy, these authors showed indeed the existence of two kinds of iron species below 200 K: the well-known Fe^{3+} and the unusual Fe^{5+}. The ordering of these species, in the form of Fe^{3+} and Fe^{5+} layers, was then determined by magnetic neutron scattering by Battle *et al.* (5): these layers are stacked along the $[111]_p$ direction of the perovskite subcell, according to the sequence "335335 …." This type of charge ordering (CO) was more recently confirmed by Li *et al.* (6) by electron microscopy.

In a recent investigation of the perovskite series $Ln_{1/3}Sr_{2/3}FeO_3$ (Ln = La, Pr, Nd, Sm, Gd) Park *et al.* (7) have confirmed the charge ordering for Ln = La, Pr, Nd as well as the antiferromagnetic spin ordering. They have shown that T_{CO} decreases with the size of the Ln^{3+} cation and finally disappears for Ln = Sm, Gd. They have interpreted this evolution as an increase of the rhombohedral distortion of the perovskite cell as the size of Ln^{3+} decreases, leading to a decrease of the electron bandwidth. Exploring the relationships between charge-ordering phenomena and magnetoresistance properties, we have revisited the perovskite $Sm_{1/3}Sr_{2/3}FeO_3$. In contrast to Park *et al.*, we observe that the resistivity exhibits a jump at 150 K, in agreement with the magnetization, which shows a peak at the same temperature. Using electron microscopy, we show that this perovskite is charge ordered with a T_{CO} value of 110 K, significantly smaller than T_N. A comparison with the other members of the series (Ln = La, Pr, Nd) is also made, which suggests that the oxygen stoichiometry may also play a role in the charge-ordering phenomena.

EXPERIMENTAL PROCEDURES

Polycrystalline samples of $Sm_{1/3}Sr_{2/3}FeO_{3-\delta}$ were synthesized by direct solid-state reaction of Sm_2O_3, $SrCO_3$, and Fe_2O_3, mixed in stoichiometric molar proportions and initially calcined at 1000°C in air. After regrinding, the resulting powder was pressed into pellets and sintered at 1400°C for 12 h. The process was repeated two times, and compounds were then annealed in air at 800°C for 3 days

[1] To whom correspondence should be addressed.

0022-4596/00 $35.00

and slowly cooled to room temperature. The resulting pellets were annealed under oxygen pressure (100 bar) at 600°C for 24 h and then subsequently cooled at 20°C/h to room temperature. Redox titration allowed the oxygen content to be determined, leading to the composition $Sm_{1/3}Sr_{2/3}FeO_{2.95}$. The resistivity of samples as a function of magnetic field (perpendicular to the probing current) and temperature was measured by the four-probe contact method, using the Physical Properties Measurement System (PPMS) with a superconducting 7 T magnet. Magnetic properties were measured using the dc and ac SQUID system with a maximum magnetic field of 5 T. ^{57}Fe Mössbauer absorption powder spectra were recorded at 4.5 and 293 K using a conventional spectrometer with a ^{57}Co/Rh source. Isomer shift values are quoted relative to metallic α-Fe at 293 K. The electron diffraction (ED) study versus temperature and the bright/dark field imaging were carried out with a JEOL 2010 electron microscope fitted with a double-tilt cooling sample holder (± 40°C for 92 K $\leq T \leq$ 300 K). The powder X-ray diffraction analysis suggests that the samples are monophasic, but the splitting of the peaks indicates that the structure is not really rhombohedral. The actual nature of the sample is discussed on the basis of the ED results.

RESULTS AND DISCUSSION

The temperature dependence of the resistivity (Fig. 1) shows semiconductor-like behavior from 300 to 150 K, with a sudden increase of resistivity around 135 K; as T decreases, a more abrupt increase is observed below 135 K. Moreover, a hysteresis effect is observed: when the sample is warmed, the resistivity jump appears at higher temperature, 150 K. This hysteretic behavior, characteristic of a first-order transition, is different from that observed by Park *et al.* (7), who did not detect any anomaly in the semiconductor-like behavior of $Sm_{1/3}Sr_{2/3}FeO_3$. Note, however, that the resistivity jump of $Sm_{1/3}Sr_{2/3}FeO_3$ is much smoother than that observed for $La_{1/3}Sr_{2/3}FeO_3$.

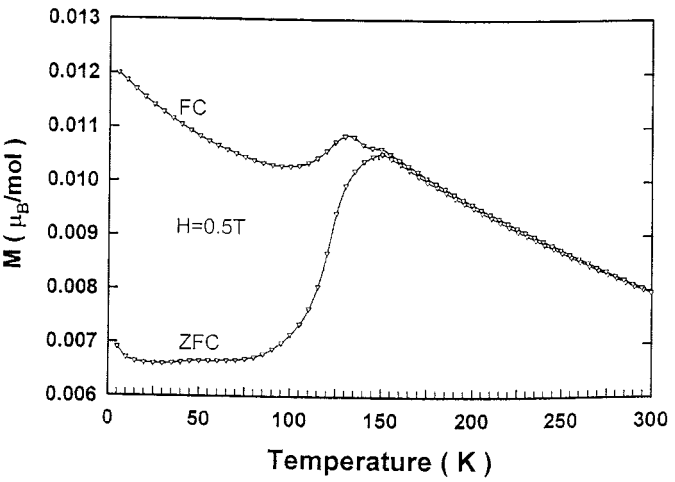

FIG. 2. Temperature dependence of the magnetization registered under 0.5 T of $Sm_{1/3}Sr_{2/3}FeO_{2.95}$. FC, field cooling; ZFC, zero field cooling.

The temperature dependence of the magnetization registered under 0.5 T (Fig. 2) clearly shows, for the zero field cooled sample, a cusp at 150 K characteristic of a paramagnetic to antiferromagnetic transition. Thus the resistive transition observed on warming (Fig. 1) coincides with $T_N = 150$ K. Moreover the field cooled sample shows a second peak at lower temperature (130 K) on the $M(T)$ curve (Fig. 2), which may be due to the formation of cluster glass domains within the AFM matrix. The ac-susceptibility curve (Fig. 3) confirms the AFM nature of the transition with a peak at $T_N = 150$ K. On return, an anomaly is detected around 130 K which cannot be explained. Nevertheless the evolution of the magnetic moment versus

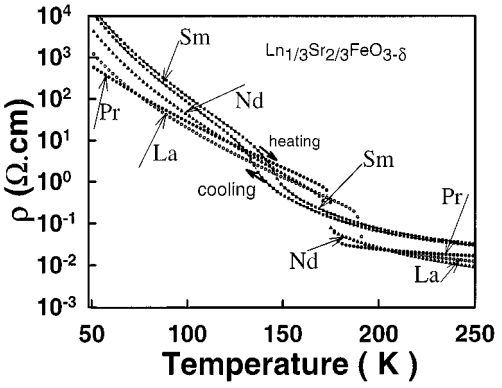

FIG. 1. Resistivity versus temperature, measurements performed as T decreases, of the $Ln_{1/3}Sr_{2/3}FeO_{3-\delta}$ series (Ln = La, Pr, Nd, Sm). To make the figure clearer, the measurements corresponding to the warming are shown only for the Sm sample.

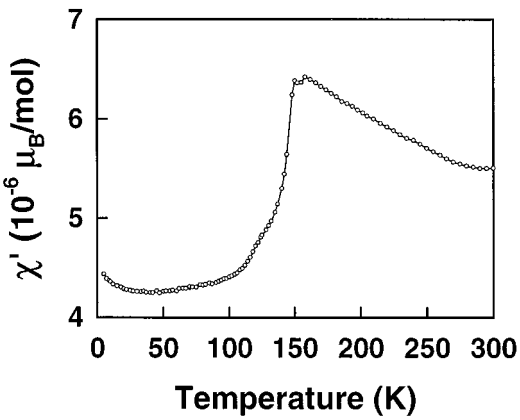

FIG. 3. Temperature dependence of the magnetic susceptibility (real part χ') of $Sm_{1/3}Sr_{2/3}FeO_{2.95}$.

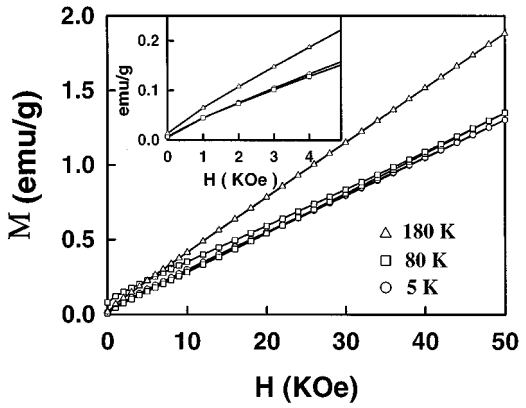

FIG. 4. Evolution of the magnetization versus magnetic field, for different temperatures, of $Sm_{1/3}Sr_{2/3}FeO_{2.95}$.

magnetic field, at different temperatures (Fig. 4), shows that at low temperature (5 K, 80 K), $M(H)$ deviates from linearity, suggesting that ferromagnetic interactions exist at low temperature, which also favor the presence of cluster glass islands within the AFM matrix. The deviation from linearity, which still persists at higher temperature (180 K) in the paramagnetic region, may result from spin fluctuations which develop short-range FM interactions.

The Mössbauer spectrum at 293 K (Fig. 5) consists of two iron components with the same quadrupole splitting value

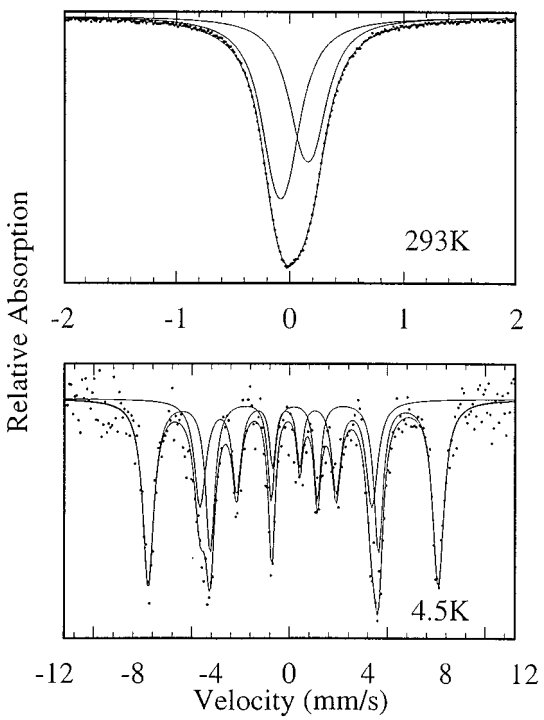

FIG. 5. ^{57}Fe Mössbauer spectra registered at 293 and 4.5 K.

(QS $\approx$ 0.11 mm/s). Although the isomer shift values are quite different (Table 1), the first one (0.27 mm/s) corresponds to the trivalent iron site and the second value (0.03 mm/s) is typical of Fe^{4+}. Note that the intensity of this Fe^{4+} component (56%) agrees with that deduced from the oxygen content ($O_{2.95}$). The Mössbauer spectrum recorded at 4.5 K (Fig. 6) shows the presence of two magnetic iron sites. The broad linewidths together with the asymmetry in the depth of the absorption lines indicate that the magnetic ordering is not well established at 4.5 K. The isomer shift (0.33 and -0.06 mm/s) and hyperfine field (46.1 and 27.2 T) values of these two sites correspond to those expected for Fe^{3+} and Fe^{5+}, respectively, in $La_{1/3}Sr_{2/3}FeO_{3-\delta}$ (8). Simultaneous inspection of relative intensities (Table 1) obtained at room (Fe^{3+}: Fe^{4+} = 44:56, EDS = 4%) and low (Fe^{3+}:Fe^{5+} = 63:37, EDS = 7%) temperatures, provides evidence that charge disproportionation could exist in our $Sm_{1/3}Sr_{2/3}FeO_{2.95}$ sample:

$$x\mathrm{Fe}^{4+} \leftrightarrow \frac{x}{2}\mathrm{Fe}^{3+} + \frac{x}{2}\mathrm{Fe}^{5+} \text{ (with } x \approx 60\%).$$

The electron diffraction investigation of the sample shows that the cell distortion is different from that of the La- and Nd-based manganites (7). The system of intense reflections is similar to the one of the rhombohedral phases, but extra reflections are systematically observed. They consist of more or less intense and weak spots, elongated along $[100]_p$*; this implies a loss of the rhombohedral symmetry. The cell parameters are $a \approx b \approx a_p\sqrt{2}$, $c \approx 2a_p$, and the conditions of reflections are consistent with the *Pbnm* space group. On these bases, the orthorhombic cell parameters at room temperature were refined from XRD patterns leading to $a = 5.4728\,(2)$ Å, $b = 5.4454\,(2)$ Å, and $c = 7.6973\,(2)$ Å. The EM images show that the two phases, rhombohedral (R-type) and orthorhombic (P-type), form small domains, embedded without any coherent boundaries. The elongated shape of the extra reflections of the $[101]_0$ ED patterns

TABLE 1

Isomer Shift (IS), Quadrupole Splitting (QS), Quadrupole Shift (2ε), Hyperfine Field (H_f), and Relative Intensity (%) of $Sm_{1/3}Sr_{2/3}FeO_{3-\delta}$ at 293 and 4.5 K

T (K)	IS ± 0.01 (mm/s)	QS ± 0.01 or 2ε ± 0.01 in magnetic phase (mm/s)	H_f ± 0.1 (T)	Iron valency	Relative intensity (%)
293	0.27	0.11	—	+ 3	44 ± 4
	0.03	0.11	—	+ 4	56 ± 4
4.5	− 0.33	− 0.05	46.1	+ 3	63 ± 7
	− 0.06	− 0.02	27.2	+ 5	37 ± 7

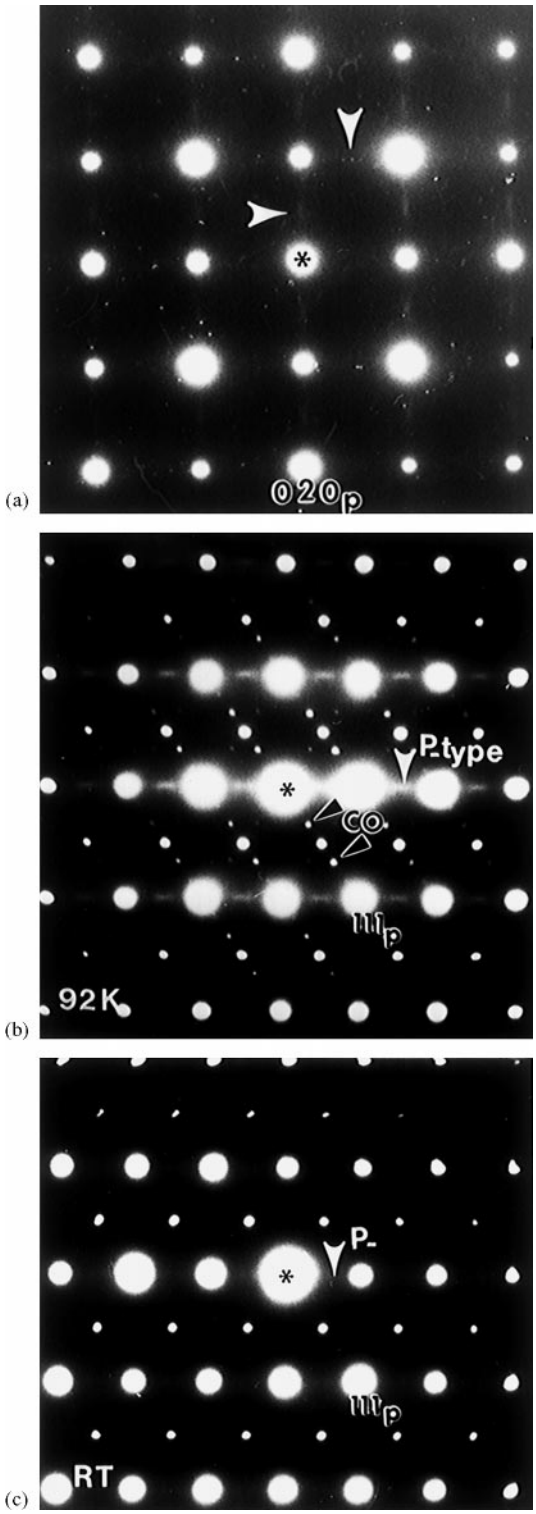

FIG. 6. (a) $[100]_p$ ED pattern recorded at room temperature. The white arrows show diffuse elongated extra reflections which are those observed in the $[101]_o$ P-type orthorhombic structure. (b) $[1\bar{1}0]_p$ ED pattern recorded at 92 K. Two sets of extra reflections are observed, generated by the P-type structure and the CO. (c) $[1\bar{1}0]_p$ ED pattern recorded after the crystal was warmed.

(Fig. 6a) is mainly due to the fact that the P-type zones occur in the form of small twinning domains, a few nanometers wide. In the diffuse streaks, nodes are sometimes visible. The result from the splitting of the *hkl*: $l = 2n + 1$ spots, due to the shape effect and complex arrangements (such as short-range ordering) of the different variants, i.e., twinning P-type and R-domains that coexist. Note that transition from *Pbnm* to $R\bar{3}c$ form is commonly observed in the perovskite manganites, by increasing T and/or Mn^{4+} content (9, 10).

At 92 K, the coexistence of P-type and R-type forms is still observed. However, another system of additional spots is evidenced. In the $[1\bar{1}0]_p$ patterns (Fig. 6b), the new satellites are indicated by black arrows. The modulation vector is parallel to $[111]_p^*$ and implies a tripling of the interreticular distance along that direction. These extra spots are similar to those previously reported in the La- and Nd-based compounds and are correlated to charge ordering (CO) (5, 7). The lattice image shows that the superstructure is established only in the R-type domains. Thus, this low-temperature form exhibits the $AB_{1/3}B'_{2/3}O_3$ ordered-type structure (11) similar to that previously described by Battle *et al.* (5) for $La_{1/3}Sr_{2/3}FeO_3$, and consequently its structure consists of an ordered arrangement of the Fe^{3+} and Fe^{5+} species, forming layers stacked along $[111]_p$ according to the sequence "335335 ...." Note also that the intensity of the P-type extra reflexions, indicated by white arrows in Fig. 6b, is reinforced at low T. This suggests that parameter variations could induce a strain effect in the interlocking domains. These results show that, when the sample is cooled at 92 K, one observes the coexistence of two phases: an ordered one, due to the transition of the R-type phase, and a distorted P-type form. When the sample is warmed, the satellites correlated to the charge ordering disappear at a temperature close to 110 K (Fig. 6c). The phenomenon is reversible.

This divergency between our results and those obtained by Park *et al.* (7) can be explained by the different experimental synthesis conditions. Our samples are polycrystalline and have been annealed under a rather high oxygen pressure of 100 bars, whereas Park's samples are crystals that were grown under an oxygen pressure of only 6 bars. Thus, it is most likely that both $Sm_{1/3}Sr_{2/3}FeO_{3-\delta}$ samples are oxygen deficient; the $\delta = 0.05$ value observed for our sample is in agreement with this viewpoint. The oxygen stoichiometry of Park's crystals and their oxygen homogeneity were unfortunately not determined (7); nevertheless, according to the oxygen pressure conditions, they might be more oxygen-deficient. It is most likely that the charge ordering and, especially, the formation of Fe^{5+} species are very sensitive to the oxygen pressure and should be favored by the application of rather high oxygen pressures. As a consequence, for our "Sm" sample, CO is achieved in large zones of the microcrystals, due to the high oxygen pressure,

whereas for Park's sample the higher oxygen deficiency hinders the Fe^{5+} formation and consequently CO is not observed. The relationships between CO and magnetotransport transitions are not straight forward, since we observe that T_{CO} (110 K) for our oxide does not coincide with T_N (150 K) but is significantly smaller. Nevertheless, it is most likely that these structural and magnetotransport properties are closely connected. The most diffuse character of the resistive and magnetic transitions observed for our $Sm_{1/3}Sr_{2/3}FeO_{3-\delta}$ sample, compared to the abrupt one observed by Park *et al.* (7) for $La_{1/3}Sr_{2/3}FeO_3$, might be related to the larger oxygen deficiency of the "Sm" sample compared to the "La" one, which would then oppose the charge disproportionation and consequently CO.

These results suggest that the size of the Ln^{3+} cation is not only factor which should affect the magnetic and transport properties of the $Ln_{1/3}Sr_{2/3}FeO_3$ perovskites. Thus a second factor, the oxygen nonstoichiometry, should also influence those properties. Consequently, the magnetotransport properties of these iron perovskites may be influenced by experimental conditions of synthesis, especially by the oxygen pressure and annealing temperatures. On the basis of these considerations, we have investigated three other oxides, $Ln_{1/3}Sr_{1/3}FeO_3$, with Ln = La, Pr, Nd. The $\rho(T)$ (Fig. 1) and $M(T)$ curves (Fig. 7) of these polycrystalline samples annealed under an oxygen pressure of 100 bars roughly confirm the results previously observed by Park *et al.* (7) concerning the coupling of the resistive and AFM transitions. We confirm that such transitions appear at 200 and 185 K for La and Pr, respectively. Nevertheless the transition of our "Pr" and "Nd" polycrystalline samples is significantly more abrupt than for Park's crystals. More importantly, a larger difference exists for the Nd polycrystalline O_2-annealed phase, which exhibits a significantly larger transition temperature ($T_N = 185$ K) than that of crystal ($T_N = 170$ K). These differences between the polycrystalline O_2-annealed oxygen samples and Park's crystals strongly support the results obtained for the Sm phase, where the oxygen nonstoichiometry is proposed to be a key factor for the appearance of charge ordering.

In conclusion, the existence of "335335 ..." charge ordering between Fe^{3+} and Fe^{5+} species has been shown for the first time in the perovskite $Sm_{1/3}Sr_{2/3}FeO_{3-\delta}$. The T_{CO} (110 K) temperature of this phase does not coincide with the magnetotransport transition, also observed for the first time ($T_N = 150$ K). Nevertheless, the two phenomena are certainly closely correlated. This behavior can be compared with that of other lanthanides (La, Pr, Nd) for both polycrystalline samples and crystals and suggest that the size of the Ln^{3+} cation is not the only parameter which governs the charge ordering in those perovskites. A second factor, the oxygen deficiency, has to be considered, which tends to hinder the Fe^{5+} formation and, consequently, to prevent CO. As consequence, the understanding of CO phenomena and of magnetotransport properties in iron perovskites requires that these compounds be considered as possibly oxygen deficient, according to the formulation $Ln_{1/3}Sr_{2/3}FeO_{3-\delta}$ and depending on the synthesis conditions.

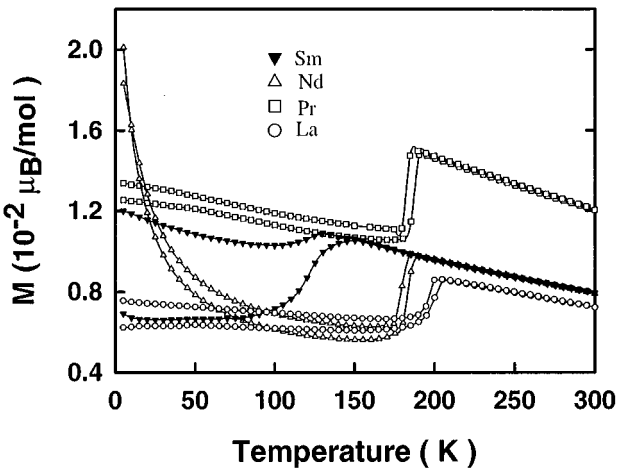

FIG. 7. Temperature dependence of the molar magnetization of $Ln_{1/3}Sr_{2/3}FeO_{3-\delta}$ series (Ln = La, Pr, Nd, Sm).

REFERENCES

1. M. Imada, A. Fujimori, and Y. Tokura, *Rev. Mod. Phys.* **70,** 1039 (1998).
2. C. N. R. Rao and B. Raveau (Eds.), "Colossal and Magnetoresistance, Charge Ordering, and Related Properties of Manganese Oxides." World Scientific, Singapore, 1998.
3. J. S. Waugh, MIT Laboratory for Insulation Research, Technical Report **No. 152.** MIT, Cambridge, MA, 1960 (unpublished).
4. M. Takano and Y. Takeda, *Bull. Inst. Chem. Kyoto Univ.* **61,** 406 (1983).
5. P. D. Battle, T. C. Gibb, and P. Lightfoot, *J. Solid State Chem.* **84,** 271 (1990).
6. J. Q. Li, Y. Matsui, S. K. Park, and Y. Tokura, *Phys. Rev. Lett.* **79**(2), 297 (1997).
7. S. K. Park, T. Ishikawa, Y. Tokura, J. Q. Li, and Y. Matsui, *Phys. Rev. B* **60,** 10788 (1999).
8. P. D. Battle, T. C. Gibb, and S. Nixon, *J. Solid State Chem.* **77,** 124 (1988).
9. F. S. Galasso, "Structure, Properties and Preparation of Perovskite Type Compounds." Pergamon Press Inc. New York, 1969.
10. A. Wold, R. J. Arnott, *J. Phys. Chem. Solids* **9,** 176 (159).
11. F. Galasso, J. R. Barrante, and L. Katz, *J. Am. Chem. Soc.* **83,** 2830 (1961).